

Tunable coherent soft X-ray source based on the generation of high-order harmonic of femtosecond laser radiation in gas-filled capillaries

Yu.A. Malkov, D.A. Yashunin, A.M. Kiselev, N.E. Andreev, A.N. Stepanov

Abstract. We have carried out experimental and theoretical investigations of a tunable coherent soft X-ray radiation source in the 30–52 nm wavelength range based on the generation of high-order harmonics of femtosecond laser radiation propagating in a dielectric xenon-filled capillary. The long path of laser pulse propagation through the capillary permits tuning the generated harmonic wavelengths to almost completely span the range under consideration.

Keywords: high-order harmonic generation, femtosecond laser radiation, gas-filled capillary.

1. Introduction

In the interaction of femtosecond laser radiation of intensity $\sim 10^{14}$ W cm⁻² with gases there occurs generation of high-order harmonics [1], i.e. of coherent radiation in the vacuum ultraviolet and soft X-ray wavelength ranges. The resultant pulsed harmonic radiation is of femtosecond duration and is spatially coherent, which permits its use in many applications like diffractometry [2], time-domain spectroscopy [3], interferometry [4] and seeding of free-electron lasers [5–7].

High-order harmonic generation is traditionally described by a three-stage model [1]: electron detachment from an atom under the action of the laser field, the oscillatory motion of electrons, and their subsequent interaction with the parent ion. The electron–ion interaction gives rise to bursts of high-frequency radiation. Among the main factors which limit the efficiency of high-order harmonic generation is the relatively short harmonics–laser radiation phase-matching length, which is due to anomalous plasma and normal gas dispersions as well as the Gouy phase shift [8, 9]. The feasibility of attaining the phase matching condition with the use of a gas-filled capillary was demonstrated in Ref. [10]. Varying the pressure in

the capillary and its related gas-induced dispersion permitted cancelling out the dispersion caused by the plasma and the existence of the capillary.

Another harmonic radiation parameter important from the standpoint of applications is the spectrum width. To obtain a broad spectrum, which is convenient for spectroscopic applications, short-pulse femtosecond lasers can be used [11]. However, even with relatively long pulses (50–100 fs in duration) it is possible to tune the harmonic wavelengths over a broad range due to a significant broadening of the spectrum of femtosecond laser pulses towards shorter wavelengths, which occurs in the propagation of laser radiation through a gas-filled capillary under ionisation [12], as well as due to a nonadiabatic spectrum shift [13] observed for very short pulses. The spectrum tuning due to the ionisation-induced shift of the laser pulse spectrum in a capillary was experimentally studied in Ref. [14], where the harmonic spectrum was tuned by varying the chirp of a 30-fs long laser pulse. However, the tuning range was limited in that work and the pressure dependences of harmonic parameters remained unexplored. Recently Butcher et al. [15] demonstrated an increase in harmonic yield and a spectrum broadening due to a nonlinear ionisation-induced self-compression during the radiation propagation in a capillary. Steingrube et al. [16] demonstrated the production of a supercontinuum in the 30–50 nm wavelength range due to a temporal pulse compression in high gas pressure filamentation. In this case, the strong absorption of harmonic radiation in the gas generates a need for a very sharp filament termination for observing the harmonics.

In the present work we carried out an experimental and theoretical investigation of the generation of high-order harmonics of the femtosecond laser radiation propagating through a gas-filled dielectric capillary. We demonstrated the feasibility of making a coherent radiation source continuously tunable in the 30–52 nm wavelength range by varying the gas pressure in the capillary and the intensity of laser radiation. We also investigated the dependences of the amplitudes, positions and spectral widths of the harmonics on the gas pressure and the intensity of laser radiation. The shift of harmonic wavelengths was shown to arise from the ionisation-induced short-wavelength shift of laser pulse spectrum, which makes it possible to achieve a substantial tuning of the X-ray radiation spectrum for a large capillary length.

2. Experimental setup

In the experiment we used a Ti:sapphire laser generating pulses of duration ~ 70 fs and energy $W = 0.5$ – 5 mJ with a pulse repetition rate of 10 Hz and a centre radiation wave-

Yu.A. Malkov, D.A. Yashunin, A.M. Kiselev Institute of Applied Physics, Russian Academy of Sciences, ul. Ul'yanova 46, 603950 Nizhnii Novgorod, Russia; e-mail: yurymalkov@mail.ru;
N.E. Andreev Joint Institute for High Temperatures, Russian Academy of Sciences, ul. Izhorskaya 13, Bld. 2, 125412 Moscow, Russia; Moscow Institute of Physics and Technology (State University), Institutskii per. 9, 141700 Dolgoprudnyi, Moscow region, Russia; e-mail: andreev@ras.ru;
A.N. Stepanov Institute of Applied Physics, Russian Academy of Sciences, ul. Ul'yanova 46, 603950 Nizhnii Novgorod, Russia; N.I. Lobachevsky Nizhnii Novgorod State University (National Research University), prosp. Gagarina 23, 603905 Nizhnii Novgorod, Russia; e-mail: step@ufp.appl.sci-nnov.ru

Received 3 March 2014; revision received 18 March 2014
 Kvantovaya Elektronika 44 (5) 484–488 (2014)
 Translated by E.N. Ragozin

length $\lambda_0 = 795$ nm. The laser beam was focused by a spherical mirror with a focal length $F = 50$ cm onto the input of a 3-cm long dielectric capillary with an inner diameter of $100 \mu\text{m}$, which was placed in a vacuum chamber with a residual pressure of less than 10^{-3} Torr (Fig. 1). The gas (xenon) was admitted into the capillary through two openings in the wall spaced at approximately 2.5 mm from its ends. The gas pressure in the capillary ranged from 0.1 to 60 Torr. The at-focus diameter of the laser beam was controlled with an aperture stop, which changed the initial beam diameter, and was so selected that only the fundamental capillary mode EH_{11} was excited. The intensity I of laser radiation at the capillary input lay in the range $(3\text{--}30) \times 10^{14} \text{ W cm}^{-2}$. We note that no apparent damage to the capillary was observed in the experiments conducted.

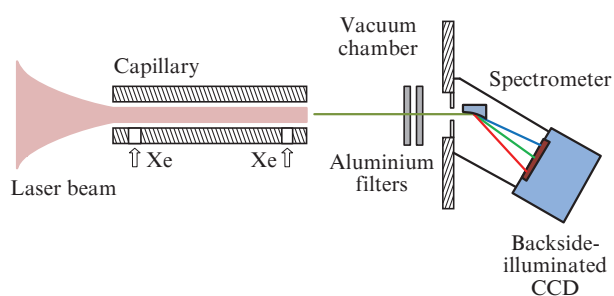


Figure 1. Scheme of the experiment.

The spectrum of high-order harmonics generated in the laser radiation–gas interaction in the capillary was diagnosed using a McPherson 248/310G spectrometer with a 600 line mm^{-1} grating and an Andor DO434-BN backside CCD for recording the X-ray radiation. The spectrometer was located at a distance $L \approx 100$ cm from the capillary output. Two $0.2\text{-}\mu\text{m}$ thick aluminium filters were placed in front of the spectrometer to protect from the optical laser radiation. In our experiment we measured the harmonic spectrum in the 30–52 nm range. The spatial distribution of the harmonics of laser radiation was measured using the same Andor CCD camera, which was accommodated in place of the spectrometer in this case.

Spectrum modifications of the laser pulses transmitted through the capillary were also investigated. To this end, the transverse laser intensity distribution at the capillary output attenuated by reflection from two glass plates was imaged with a lens onto the entrance slit of a calibrated digital spectrometer (S150 model, Solar LS). The spectrometer entrance slit width was substantially smaller than the image size, and therefore the spectrum was in fact measured in the paraxial part of the laser beam.

3. Results

When laser radiation with an intensity $I > 10^{14} \text{ W cm}^{-2}$ was focused onto the input of a xenon-filled capillary, we observed at its output an X-ray beam directed along the capillary axis. The angular beam divergence lowered with increasing pressure to become equal to several milliradians for a pressure of 15–30 Torr for a capillary $75 \mu\text{m}$ in diameter (Fig. 2).

Figure 3 shows typical harmonic spectra obtained for different gas pressures and laser radiation intensities at the capillary input. It is pertinent to note that the pressure dependences of the amplitudes of several harmonics are complex

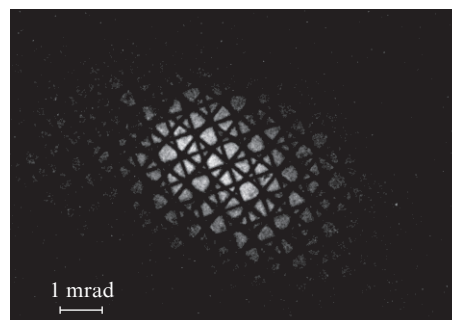


Figure 2. Angular harmonic intensity distribution at the capillary output. The dark mesh is produced by the support structure of aluminium filters, which serve to reject optical radiation.

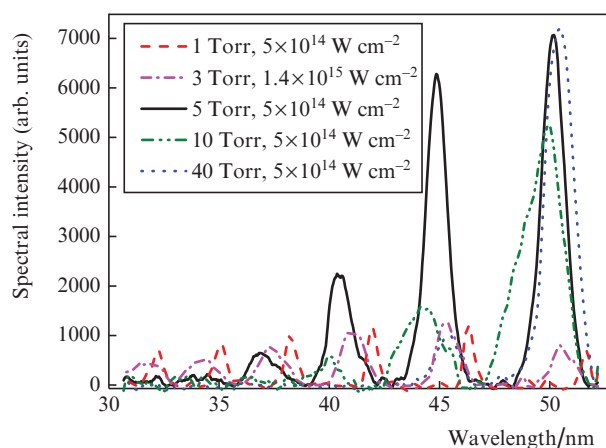


Figure 3. High-order harmonic spectrum for different gas pressures and laser radiation intensities.

and nonmonotonic. The second important feature consists in appreciable wavelength shifts of individual harmonics; in the context of our experiment it allowed spanning almost completely the 30–52 nm wavelength range. This circumstance is of major significance for spectroscopic investigations.

The energies and relative spectral shifts λ_n/λ_{0n} (where $\lambda_{0n} = \lambda_0/n$) for harmonics with numbers $n = 15\text{--}25$ generated in the capillary are plotted in Figs 4 and 5 as functions of laser radi-

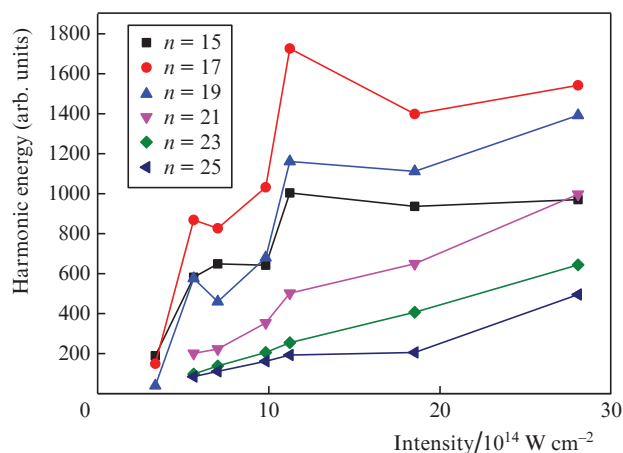


Figure 4. Intensity dependences of harmonic energies for a pressure of 3 Torr.

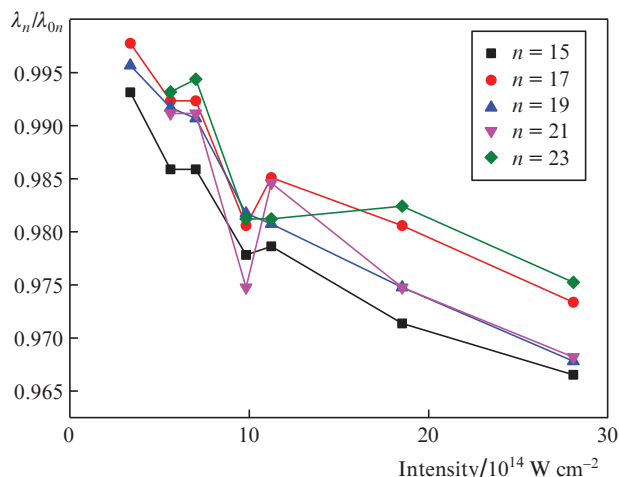


Figure 5. Intensity dependence of the relative harmonic spectral shifts for a pressure of 3 Torr.

ation intensity at the capillary input for a 3-Torr gas pressure in the capillary. At moderate intensities the lower-order harmonics exhibited a rapid growth of harmonic signals, which was subsequently replaced by saturation. Higher-order harmonics (beginning with the 19th) show a slow increase in harmonic amplitudes with increasing laser radiation intensity. We also observed the increase in the shift of the harmonic spectrum with increasing intensity. We note that the spectrum shifts of all harmonics measured in our experiment exhibited similar intensity dependences.

The dependence of individual harmonic parameters on the xenon pressure in the capillary was also measured in the experiment. Figure 6 shows the pressure dependences of harmonic energies, which exhibit a nonmonotonic behaviour. A sharp energy growth is observed at low pressures. In the 3–5 Torr region the harmonic signals attain their maxima, which shift towards higher pressures with lowering the harmonic number n . A secondary intensity growth is observed at higher pressures for harmonics with $n = 15$ and 17, while the high-order harmonics with $n > 19$ vanish.

The centre-of-mass positions of the spectra of radiated harmonics appreciably and simultaneously shift towards shorter

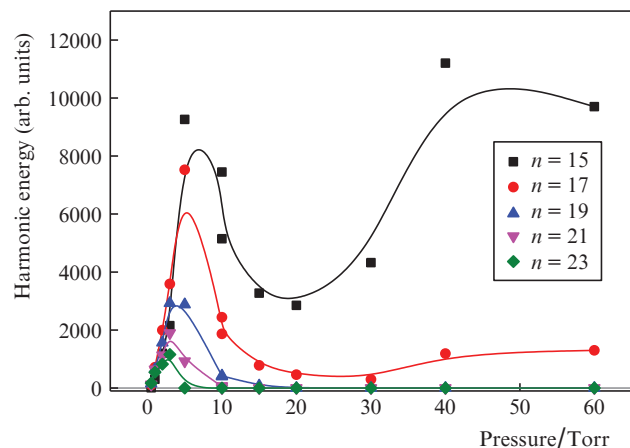


Figure 6. Harmonic energies as functions of gas pressure for an intensity of $10^{15} \text{ W cm}^{-2}$.

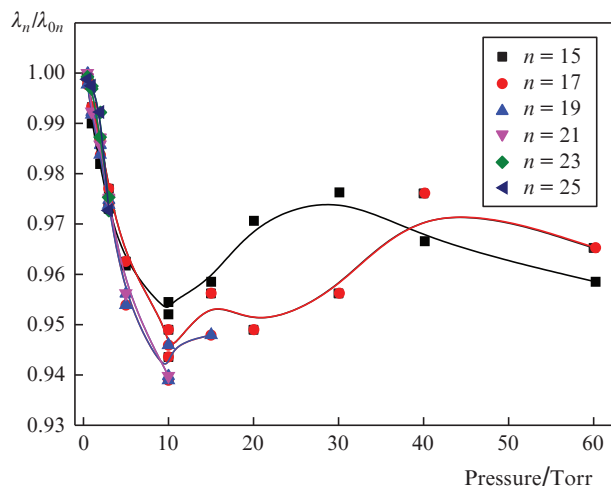


Figure 7. Relative harmonic spectral shifts as functions of gas pressure for an intensity of $10^{15} \text{ W cm}^{-2}$.

wavelengths with increasing pressure (Fig. 7); the spectrum shift saturates at pressures above 10 Torr.

4. Discussion and numerical simulations

The dependence of harmonic energies on the intensity of laser radiation (Fig. 4) may be interpreted as follows. At a low intensity (below $3 \times 10^{14} \text{ W cm}^{-2}$), when the degree of gas ionisation is small and the resultant plasma has only a slight effect on the propagation of laser radiation, the lower-order harmonics exhibit a rapid growth due to a sharp intensity dependence of the ionisation probability. At higher intensities, the capillary plasma lowers the capillary's transmittance to the laser radiation, which leads to a significant moderation of the growth of harmonic amplitudes or the complete saturation of the dependences. The increase in harmonic spectral shifts with increasing laser intensity (Fig. 5) is quite consistent with the model of short-wavelength modification of the spectrum of a laser pulse, which becomes stronger with increasing intensity.

A qualitative model of harmonic generation was developed earlier in Refs [10, 17]; it takes into account the phase matching between the laser radiation and its harmonics, ionisation, absorption of laser radiation in the gas and plasma, and the existence of a limiting harmonic number, so that no X-ray harmonics with higher numbers are generated. Proceeding from this model we calculated the dependences of harmonic characteristics on the gas pressure in the capillary. It showed that the maxima of harmonic amplitudes are indeed observed in the 1–10 Torr range and are similar to those displayed in Fig. 6. The inclusion of the dispersion of X-ray radiation in the gas permits explaining the pressure shifts of the different harmonics maxima towards higher pressures with a decrease in harmonic number. We note that the qualitative agreement between the shape of the pressure dependences of harmonic amplitudes and our experimental data was reached assuming a high degree of gas ionisation in the capillary, which resulted in a strong plasma influence on the dispersion. This statement is consistent with an estimate of xenon ionisation under the laser intensities employed in the experiment and with the results of numerical simulations outlined below.

As is well known, in the propagation of femtosecond laser pulses through an extended path under ionisation conditions there occurs a significant short-wavelength broadening of the

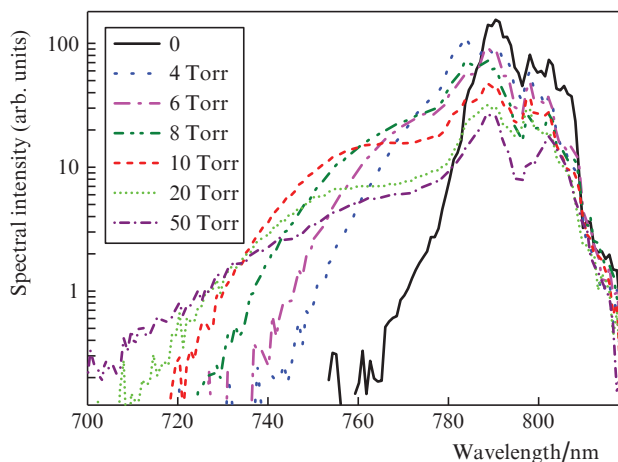


Figure 8. Spectra of laser pulses for different pressures for an intensity of $5 \times 10^{14} \text{ W cm}^{-2}$.

spectrum of the laser pulses [12]. This stems from the frequency variation occurring in the radiation propagation through a transient medium with the refractive index decreasing in time. This effect was also observed experimentally in the present work (Fig. 8). With increasing gas pressure in the capillary the spectrum of laser pulses is broadened down to 700 nm. Figure 9 shows the pressure dependence of the centre-of-mass position of the pulse spectrum obtained by processing the data of Fig. 8. One can see that there occurs a sharp shortening of the average wavelength followed by its saturation as the pressure is increased to 10 Torr.

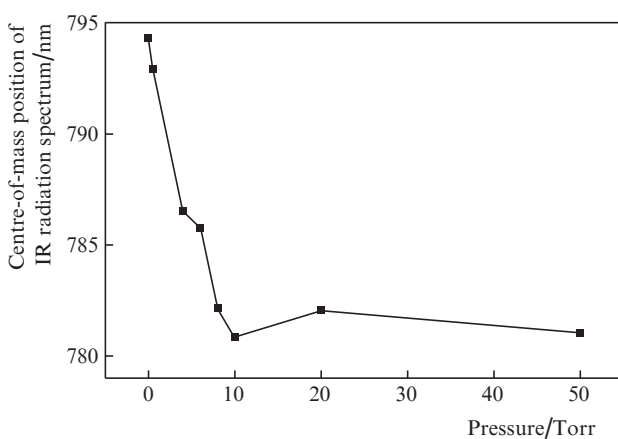


Figure 9. Shift of laser radiation spectrum as a function of pressure.

When propagating through the capillary, a laser pulse continuously generates high-order harmonics. However, because of the high X-ray absorption coefficient in the gas at a pressure higher than several Torr, the harmonics are efficiently produced only in the capillary portion closest to the capillary end, where the laser radiation spectrum is blue-shifted, in accordance with the data depicted in Fig. 9. This gives rise to the corresponding shift of the harmonic spectrum towards shorter wavelengths.

A comparison of Figs 7 and 9 suggests that the pressure dependence of the shift of laser radiation spectrum virtually reproduces the pressure dependence of individual harmonic

wavelengths: at low pressures the spectrum shifts to shorter wavelengths and at pressures above 10 Torr there occurs saturation. This allows a conclusion that the observed short-wavelength shift of harmonic spectra is caused by precisely the ionisation-induced ‘blue’ shift of the spectrum of the driving laser pulse.

It is significant that the experimentally measured capillary transmittance to the laser radiation decreases considerably with increasing pressure (Fig. 10). This is caused by the radiation loss for ionisation and the radiation scattering to higher-order higher-loss capillary modes [18, 19] from plasma density nonuniformities. The lowering of transmittance results in a decrease in laser intensity at the capillary output and, in particular, leads to a suppression of the high-order harmonic generation observed in Fig. 6. The latter is attributable to the fact that the highest harmonic photon energy, according to the three-stage harmonic generation model [1], does not exceed a value $I_p + 3.17U_p$, where I_p is the ionisation potential of the atom (ion); $U_p = e^2 E^2 / (4m_e \omega^2)$ is the electron oscillatory energy; e and m_e are the electron charge and mass; and E and ω are the amplitude and frequency of the laser field. The lowering of laser radiation intensity with gas pressure also results in a lowering of gas ionisation rate and the consequential saturation of the ‘blue’ shift observed in Fig. 9.

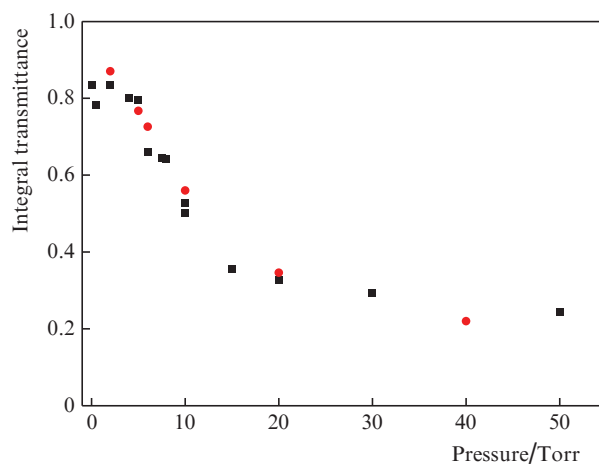


Figure 10. Experimental (■) and theoretical (●) dependences of capillary transmittance to laser radiation on the pressure.

To analyse our experimental data, we performed numerical simulations of the propagation of laser pulses through a gas-filled capillary in an axially-symmetric geometry with the inclusion of ionisation. The dynamics of field-ionised plasma production by a short high-intensity laser pulse was described by the system of kinetic equations of sequential ionisation of the atoms (ions). The tunnel ionisation probability corresponded to the Ammosov–Delone–Krainov model. The propagation of laser radiation through the nonlinear transient medium was described using a wave equation, which included the optical field ionisation of the gas by laser pulses and the temporal laser pulse dispersion as well as the relativistic and ponderomotive nonlinearities of the plasma produced by the high-intensity radiation [20–23].

Our numerical simulations yielded the transmittance as well as the temporal shape and spectrum of laser pulses at the capillary output. The calculated data for integral capillary

transmittance to the laser radiation and the corresponding experimental data are given in Fig. 10, which shows their excellent agreement.

The spectral characteristics of output laser radiation depend heavily on the details of the temporal structure and spectrum of the initial laser pulse. The spectrum of the laser pulse measured in the absence of gas in the capillary (Fig. 8) shows a clearly defined long-wavelength wing, which also manifests itself in the spectrum of the pulse transmitted through the gas-filled capillary (the solid curve in Fig. 11). In our simulations the pulse at the capillary input was assumed to be Gaussian-shaped and, consequently, had a symmetric spectrum with a half-amplitude width corresponding to the spectral width of the initial measured pulse. The simulated spectrum of the pulse transmitted through the gas-filled capillary is shown in Fig. 11 for a gas pressure of 10 Torr. The transmitted radiation spectrum obtained in the simulations reproduces rather well the formation of the ‘blue’ wing of the spectrum, which is caused primarily by the gas ionisation in the capillary.

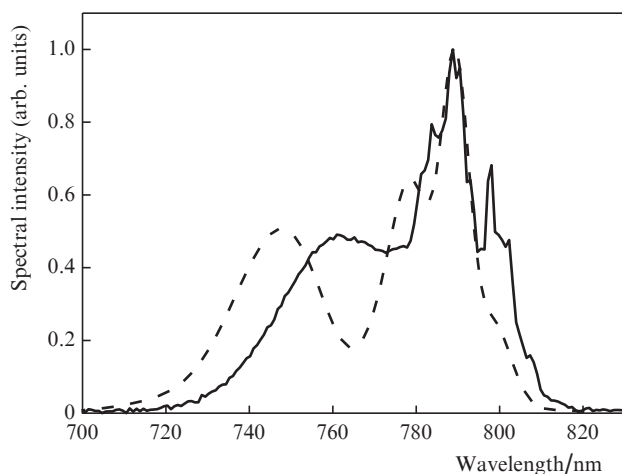


Figure 11. Experimental (solid curve) and theoretical (dashed curve) spectra at the capillary output at a pressure of 10 Torr.

5. Conclusions

We have performed experimental and theoretical investigations of a coherent soft X-ray radiation source in the 30–52 nm wavelength range, which is based on the generation of harmonics of titanium-sapphire femtosecond laser radiation propagating through a xenon-filled dielectric capillary. Despite the relatively long duration of the laser pulse, by varying its energy and the gas pressure it has been possible to obtain a soft X-ray radiation source tunable almost continuously in the wavelength range under consideration. The tuning of the harmonic spectrum is determined by the ionisation-induced shift of the spectrum of laser radiation due to a relatively long capillary length, which is borne out by experimental measurements as well as by our numerical simulations of the high-intensity laser pulse propagation through the capillary.

Acknowledgements. This work was supported by the Presidium of the Russian Academy of Sciences in the framework of the Programme ‘Extreme Light Fields and Their Applications’.

References

- Lewenstein M., Balcou P., Ivanov M.Yu., L’Huillier A., Corkum P.B. *Phys. Rev. A*, **49**, 2117 (1994).
- Sandberg R.L., Paul A., Raymondson D.A., Hädrich S., Gaudiosi D.M., Holtsnider J., Ra’anan I.T., Cohen O., Murnane M.M., Kapteyn H.C. *Phys. Rev. Lett.*, **99**, 098103 (2007).
- Wörner H., Bertrand J., Fabre B., Higuier J., Ruf H., Dubrouil A., Patchkovskii S., Spanner M., Mairesse Y., Blanchet V. *Science*, **334**, 208 (2011).
- Descamps D., Lyngå C., Norin J., L’Huillier A., Wahlström C.-G., Hergott J.-F., Merdji H., Salières P., Bellini M., Hänsch T. *Opt. Lett.*, **25**, 135 (2000).
- Lambert G., Hara T., Garzella D., Tanikawa T., Labat M., Carre B., Kitamura H., Shintake T., Bougeard M., Inoue S. *Nat. Phys.*, **4**, 296 (2008).
- Togashi T., Takahashi E.J., Midorikawa K., Aoyama M., Yamakawa K., Sato T., Iwasaki A., Owada S., Okino T., Yamanouchi K. *Opt. Express*, **19**, 317 (2011).
- Ardana-Lamas F., Lambert G., Trisorio A., Vodungbo B., Malka V., Zeitoun P., Hauri C. *New J. Phys.*, **15**, 073040 (2013).
- L’Huillier A., Schafer K., Kulander K. *Phys. Rev. Lett.*, **66**, 2200 (1991).
- L’Huillier A., Li X., Lompré L. *J. Opt. Soc. Am. B*, **7**, 527 (1990).
- Durfee III C.G., Rundquist A.R., Backus S., Herne C., Murnane M.M., Kapteyn H.C. *Phys. Rev. Lett.*, **83**, 2187 (1999).
- Goulielmakis E., Schultze M., Hofstetter M., Yakovlev V., Gagnon J., Uiberacker M., Aquila A., Gullikson E., Attwood D., Kienberger R. *Science*, **320**, 1614 (2008).
- Babin A., Kartashov D., Kiselev A., Lozhkarev V., Stepanov A., Sergeev A. *Appl. Phys. B*, **75**, 509 (2002).
- Shin H.J., Lee D.G., Cha Y.H., Hong K.H., Nam C.H. *Phys. Rev. Lett.*, **83**, 2544 (1999).
- Froud C.A., Rogers E.T., Hanna D.C., Brocklesby W.S., Praeger M., de Paula A.M., Baumberg J.J., Frey J.G. *Opt. Lett.*, **31**, 374 (2006).
- Butcher T., Anderson P., Chapman R., Horak P., Frey J.G., Brocklesby W. *Phys. Rev. A*, **87**, 043822 (2013).
- Steingrube D., Schulz E., Binhammer T., Gaarde M., Couairon A., Morgner U., Kovačev M. *New J. Phys.*, **13**, 043022 (2011).
- Rogers E.T., Stebbings S.L., de Paula A.M., Froud C.A., Praeger M., Mills B., Grant-Jacob J., Brocklesby W.S., Frey J.G. *J. Opt. Soc. Am. B*, **29**, 806 (2012).
- Marcatili E., Schmeltzer R. *Bell System Tech. J.*, **43**, 1783 (1964).
- Cros B., Courtois C., Matthieussent G., Di Bernardo A., Batani D., Andreev N., Kuznetsov S. *Phys. Rev. E*, **65**, 026405 (2002).
- Andreev N., Nishida Y., Yugami N. *Phys. Rev. E*, **65**, 056407 (2002).
- Andreev N., Cros B., Gorbunov L., Matthieussent G., Mora P., Ramazashvili R. *Phys. Plasmas*, **9**, 3999 (2002).
- Andreev N., Cassou K., Wojda F., Genoud G., Burza M., Lundh O., Persson A., Cros B., Fortov V., Wahlstrom C. *New J. Phys.*, **12**, 045024 (2010).
- Eremin V., Malkov Yu., Korolikhin V., Kiselev A., Skobelev S., Stepanov A., Andreev N. *Phys. Plasmas*, **19**, 093121 (2012).